Periodic Orbit Quantization: How to Make Semiclassical Trace Formulae Convergent*

Jörg Main and Günter Wunner
Institut für Theoretische Physik I, Universität Stuttgart, D-70550 Stuttgart, Germany
(February 8, 2008)

Abstract

Periodic orbit quantization requires an analytic continuation of non-convergent semiclassical trace formulae. We propose two different methods for semiclassical quantization. The first method is based upon the harmonic inversion of semiclassical recurrence functions. A band-limited periodic orbit signal is obtained by analytical frequency windowing of the periodic orbit sum. The frequencies of the periodic orbit signal are the semiclassical eigenvalues, and are determined by either linear predictor, Padé approximant, or signal diagonalization. The second method is based upon the direct application of the Padé approximant to the periodic orbit sum. The Padé approximant allows the resummation of the, typically exponentially, divergent periodic orbit terms. Both techniques do not depend on the existence of a symbolic dynamics, and can be applied to bound as well as to open systems. Numerical results are presented for two different systems with chaotic and regular classical dynamics, viz. the three-disk scattering system and the circle billiard.

PACS numbers: 05.45.−a, 03.65.Sq

*Contribution to "Festschrift in honor of Martin Gutzwiller", eds. A. Inomata et al., to be published in *Foundations of Physics*.

I. INTRODUCTION

Semiclassical periodic orbit quantization is a nontrivial problem for the reason that Gutzwiller's trace formula [1,2] for chaotic systems and the Berry-Tabor formula [3] for integrable systems do not usually converge in those regions where the physical eigenenergies or resonances are located. Various techniques have been developed to circumvent the convergence problem of periodic orbit theory. Examples are the cycle expansion technique [4], the Riemann-Siegel type formula and pseudo-orbit expansions [5], surface of section techniques [6], and a quantization rule based on a semiclassical approximation to the spectral staircase [7]. These specific techniques have proven to be very efficient for individual systems with special properties, e.g., the cycle expansion for hyperbolic systems with an existing symbolic dynamics. The other methods mentioned have been used for the calculation of bound spectra of specific systems.

Recently, an alternative method based upon filter-diagonalization (FD) has been introduced for the analytic continuation of the semiclassical trace formula [8,9]. The FD method requires knowledge of the periodic orbits up to a given maximum period (classical action), which depends on the mean density of states. The semiclassical eigenenergies or resonances are obtained by *harmonic inversion* of the periodic orbit recurrence signal. The FD method can be generally applied to both open and bound systems and has also proven to be a powerful tool, e.g., for the calculation of semiclassical transition matrix elements [10] and the quantization of systems with mixed regular-chaotic phase space [11]. For a review on periodic orbit quantization by harmonic inversion see [12].

In this paper we present two different techniques to make semiclassical periodic orbit sums convergent. The first method is an advanced version of harmonic inversion adapted to the special structure of periodic orbit signals given as sums of δ functions [13]. The semiclassical signal, in action or time, corresponds to a "spectrum" or response in the frequency domain that is composed of a huge, in principle infinite, number of frequencies. To extract these frequencies and their corresponding amplitudes is a nontrivial task. In previous work [8,9,12] the periodic orbit signal has been harmonically inverted by means of FD [14–16] which is designed for the analysis of time signals given on an equidistant grid. The periodic orbit recurrence signal is represented as a sum over usually unevenly spaced δ functions. A smooth signal, from which evenly spaced values can be read off, is obtained by a convolution of this sum with, e.g., a narrow Gaussian function. The disadvantages of this approach are twofold. Firstly, FD acts on this signal more or less like a "black box" and, as such, does not lend itself to a detailed understanding of semiclassical periodic orbit quantization. Secondly, the smoothed semiclassical signal usually consists of a huge number of data points. The handling of such large data sets, together with the smoothing, may lead to significant numerical errors in results for the semiclassical eigenenergies and resonances. Here, we propose alternative techniques for the harmonic inversion of the periodic orbit recurrence signal that avoid these problems. In a first step we create a shortened signal which is constructed from the original signal and designed to be correct only in a window, i.e., a short frequency range of the total band width. Because the original signal is given as a periodic orbit sum of δ functions, this "filtering" can be performed analytically resulting in a band-limited periodic orbit signal with a relatively small number of equidistant grid points. In a second step the frequencies and amplitudes of the band-limited signal are determined from a set of nonlinear equations.

To solve the nonlinear system, we introduce three different processing methods, viz. linear predictor (LP), Padé approximant (PA), and signal diagonalization (SD). It is important to note that these processing methods would not have yielded numerically stable solutions if the signal had not first been band-limited by the windowing (filtering) procedure. Furthermore, this separation of the harmonic inversion procedure into various steps may elucidate a clearer picture of the periodic orbit quantization method itself, and even provides more accurate results than previous calculations [9,12] using FD.

The second method is the direct application of the Padé approximant to slowly convergent and/or divergent periodic orbit sums [17]. In the former or the latter case, the PA either significantly increases the convergence rate, or analytically continues the *exponentially* divergent series, respectively. The PA is especially robust for resumming diverging series in many applications in mathematics and theoretical physics [18]. An important example is the summation of the divergent Rayleigh-Schrödinger quantum mechanical perturbation series, e.g., for atoms in electric [19] and magnetic [20] fields. In periodic orbit theory the PA has been applied to cycle-expanded Euler products and dynamical zeta functions [21]. It should be noted that the Padé approximant is applied in both methods in a completely different context, namely, in the first method as a tool for signal processing [13,22], and in the second for the direct summation of the periodic orbit terms in the semiclassical trace formulae.

In Sec. II we present our first method to make semiclassical trace formulae convergent. After briefly reviewing the general idea of periodic orbit quantization by harmonic inversion in Sec. II A we construct, in Sec. II B, the band-limited periodic orbit signal which is analyzed, in Sec. II C, with the help of either LP, PA, or SD. In Sec. III we introduce our second method for semiclassical quantization, viz. the direct application of the Padé approximant to the periodic orbit sum. In Sec. IV we present and compare results for the three-disk repeller and the circle billiard as physical examples of relevance. A few concluding remarks are given in Sec. V.

II. HARMONIC INVERSION OF PERIODIC ORBIT SIGNALS

A. General remarks

In order to understand what follows, a brief recapitulation of the basic ideas of periodic orbit quantization by harmonic inversion may be useful. For further details see [12].

Following Gutzwiller [1,2] one can write the semiclassical response function for chaotic systems in the form

$$g^{\mathrm{sc}}(E) = g_0^{\mathrm{sc}}(E) + \sum_{\mathrm{po}} \mathcal{A}_{\mathrm{po}} \mathrm{e}^{\mathrm{i}S_{\mathrm{po}}} \ , \tag{1}$$

where $g_0^{\mathrm{sc}}(E)$ is a smooth function and S_{po} and $\mathcal{A}_{\mathrm{po}}$ are the classical actions and weights (including phase information given by the Maslov index) of the periodic orbit (po) contributions. Equation (1) is also valid for integrable systems when the periodic orbit quantities are calculated not with Gutzwiller's trace formula, but with the Berry-Tabor formula [3] for periodic orbits on rational tori. The eigenenergies and resonances are the poles of the response function. Unfortunately, the semiclassical approximation (1) does not converge in

the region of the poles, and hence one is faced with the problem of the analytic continuation of $g^{\rm sc}(E)$ to this region.

As in previous work [8,9,12], we will make the (weak) assumption that the classical system has a scaling property, i.e., the shape of periodic orbits is assumed not to depend on a scaling parameter, w, and the classical action scales as

$$S_{\rm po} = w s_{\rm po} \ . \tag{2}$$

In scaling systems, the fluctuating part of the semiclassical response function,

$$g^{\rm sc}(w) = \sum_{\rm po} \mathcal{A}_{\rm po} {\rm e}^{{\rm i}w s_{\rm po}} \ , \tag{3}$$

can be Fourier transformed readily to yield the semiclassical trace of the propagator

$$C^{\rm sc}(s) = \frac{1}{2\pi} \int_{-\infty}^{+\infty} g^{\rm sc}(w) {\rm e}^{-{\rm i}sw} {\rm d}w = \sum_{\rm po} \mathcal{A}_{\rm po} \delta \left(s - s_{\rm po} \right) \ . \tag{4}$$

The signal $C^{\rm sc}(s)$ has δ spikes at the positions of the classical periods (scaled actions) $s = s_{\rm po}$ of periodic orbits and with peak heights (recurrence strengths) $\mathcal{A}_{\rm po}$, i.e., $C^{\rm sc}(s)$ is Gutzwiller's periodic orbit recurrence function. Consider now the quantum mechanical counterparts of $g^{\rm sc}(w)$ and $C^{\rm sc}(s)$ taken as the sums over the poles w_k of the Green's function,

$$g^{\rm qm}(w) = \sum_k \frac{d_k}{w - w_k + {\rm i}\epsilon} \ , \tag{5}$$

$$C^{\rm qm}(s) = \frac{1}{2\pi} \int_{-\infty}^{+\infty} g^{\rm qm}(w) {\rm e}^{-{\rm i}sw} {\rm d}w = -{\rm i} \sum_k d_k {\rm e}^{-{\rm i}w_k s} \ , \tag{6}$$

with d_k being the residues associated with the eigenvalues. In the case under study, i.e., density of states spectra, the d_k are the multiplicities of eigenvalues and are equal to 1 for non-degenerate states. Semiclassical eigenenergies w_k and residues d_k can now, in principle, be obtained by adjusting the semiclassical signal, Eq. (4), to the functional form of the quantum signal, Eq. (6), with the $\{w_k, d_k\}$ being free, in general complex, frequencies and amplitudes. This scheme is known as "harmonic inversion". The numerical procedure of harmonic inversion is a nontrivial task, especially if the number of frequencies in the signal is large (e.g., more than a thousand), or even infinite as is usually the case for periodic orbit quantization. Note that the conventional way to perform the spectral analysis, i.e., the Fourier transform of Eq. (4) will bring us back to analyzing the non-convergent response function $g^{\rm sc}(w)$ in Eq. (3). The periodic orbit signal (4) can be harmonically inverted by application of FD [14–16], which allows one to calculate a finite and relatively small set of frequencies and amplitudes in a given frequency window. The usual implementation of FD requires knowledge of the signal on an equidistant grid. The signal (4) is not a continuous function. However, a smooth signal can be obtained by a convolution of $C^{\rm sc}(s)$ with, e.g., a Gaussian function,

$$C^{\rm sc}_\sigma(s) = \frac{1}{\sqrt{2\pi}\sigma} \sum_{\rm po} \mathcal{A}_{\rm po} {\rm e}^{-(s-s_{\rm po})^2/2\sigma^2} \ . \tag{7}$$

As can easily be seen, the convolution results in a damping of the amplitudes, $d_k \to d_k^{(\sigma)} = d_k \exp(-w_k^2\sigma^2/2)$. The width σ of the Gaussian function should be chosen sufficiently small to avoid an overly strong damping of amplitudes. To properly sample each Gaussian a dense grid with steps $\Delta s \approx \sigma/3$ is required. Therefore, the signal (7) analyzed by FD usually consists of a large number of data points. The numerical treatment of this large data set may suffer from rounding errors and loss of accuracy. Additionally, the "black box" type procedure of harmonic inversion by FD, which intertwines windowing and processing, does not provide any opportunity to gain a deeper understanding of semiclassical periodic orbit quantization. It is therefore desirable to separate the harmonic inversion procedure into two sequential steps: Firstly, the filtering procedure that does not require smoothing and, secondly, a procedure for extracting the frequencies and amplitudes. In Sec. II B we will construct, by analytic filtering, a band-limited signal which consists of a relatively small number of frequencies. In Sec. II C we will present methods to extract the frequencies and amplitudes of such band-limited signals.

B. Construction of band-limited signals by analytical filtering

In general, a frequency filter can be applied to a given signal by application of the Fourier transform [22–24]. The signal is transformed to the frequency domain, e.g., by application of the fast Fourier transform (FFT) method. The transformed signal is multiplied with a frequency filter function $f(w)$ localized around a central frequency, w_0. The frequency filter $f(w)$ can be rather general, typical examples are a rectangular window or a Gaussian function. The filtered signal is then shifted by $-w_0$ and transformed back to the time domain by a second application of FFT. The filtered signal consists of a significantly reduced set of frequencies, and therefore a reduced set of grid points is sufficient for the analysis of the signal. This technique is known as "beam spacing" [23] or "decimation" [22,24] of signals.

The special form of the periodic orbit signal (4) as a sum of δ functions allows for an even simpler procedure, viz. analytical filtering. In the following we will apply a rectangular filter, i.e., $f(w) = 1$ for frequencies $w \in [w_0 - \Delta w, w_0 + \Delta w]$, and $f(w) = 0$ outside the window. The generalization to other types of frequency filters is straightforward. Starting from the semiclassical response function (spectrum) $g^{\rm sc}(w)$ in Eq. (3), which is itself a Fourier transform of the "signal" (4), and using a rectangular window we obtain, after evaluating the "second" Fourier transform, the band-limited (bl) periodic orbit signal,

$$\begin{aligned} C_{\rm bl}^{\rm sc}(s) &= \frac{1}{2\pi}\int_{w_0-\Delta w}^{w_0+\Delta w} g^{\rm sc}(w)\mathrm{e}^{-\mathrm{i}s(w-w_0)}\mathrm{d}w \\ &= \frac{1}{2\pi}\sum_{\rm po}\mathcal{A}_{\rm po}\int_{w_0-\Delta w}^{w_0+\Delta w}\mathrm{e}^{\mathrm{i}sw_0-\mathrm{i}(s-s_{\rm po})w}\mathrm{d}w \\ &= \sum_{\rm po}\mathcal{A}_{\rm po}\frac{\sin\left[(s-s_{\rm po})\Delta w\right]}{\pi(s-s_{\rm po})}\mathrm{e}^{\mathrm{i}s_{\rm po}w_0}\ . \end{aligned} \tag{8}$$

The introduction of w_0 into the arguments of the exponential functions in (8) causes a shift of frequencies by $-w_0$ in the frequency domain. Note that $C_{\rm bl}^{\rm sc}(s)$ is a smooth function and can be easily evaluated on an arbitrary grid of points $s_n < s_{\rm max}$ provided the periodic orbit data are known for the set of orbits with classical action $s_{\rm po} < s_{\rm max}$.

Applying now the same filter as used for the semiclassical periodic orbit signal to the quantum one, we obtain the band-limited quantum signal

$$C_{\rm bl}^{\rm qm}(s) = \frac{1}{2\pi}\int_{w_0-\Delta w}^{w_0+\Delta w} g^{\rm qm}(w)\mathrm{e}^{-\mathrm{i}s(w-w_0)}\mathrm{d}w$$
$$= -\mathrm{i}\sum_{k=1}^{K} d_k \mathrm{e}^{-\mathrm{i}(w_k-w_0)s} \ , \quad |w_k - w_0| < \Delta w \ . \tag{9}$$

In contrast to the signal $C^{\rm qm}(s)$ in Eq. (6), the band-limited quantum signal consists of a *finite* number of frequencies w_k, $k = 1, \ldots, K$, where in practical applications K can be of the order of $\sim$ (50-200) for an appropriately chosen frequency window, Δw. The problem of adjusting the band-limited semiclassical signal in Eq. (8) to its quantum mechanical analogue in Eq. (9) can now be written as a set of $2K$ nonlinear equations

$$C_{\rm bl}^{\rm sc}(n\tau) \equiv c_n = -\mathrm{i}\sum_{k=1}^{K} d_k \mathrm{e}^{-\mathrm{i}w'_k n\tau} \ , \quad n = 0, 1, \ldots, 2K-1 \ , \tag{10}$$

for the $2K$ unknown variables, viz. the shifted frequencies, $w'_k \equiv w_k - w_0$, and amplitudes, d_k. The band-limited signal now becomes "short"as it can be evaluated on an equidistant grid, $s = n\tau$, with relatively large step width $\tau \equiv \pi/\Delta w$. It is important to note that the number of signal points c_n in Eq. (10) is usually much smaller than a reasonable discretization of the signal $C_\sigma^{\rm sc}(s)$ in Eq. (7), which is the starting point for harmonic inversion by FD. Therefore, the discrete signal points $c_n \equiv C_{\rm bl}^{\rm sc}(n\tau)$ are called the "band-limited" periodic orbit signal. Methods to solve the nonlinear system, Eq. (10), are discussed in Sec. II C below.

It should also be noted that the analytical filtering in Eq. (8) is not restricted to periodic orbit signals, but can be applied, in general, to any signal given as a sum of δ functions. An example is the high resolution analysis of quantum spectra [12,25,26], where the density of states is $\varrho(E) = \sum_n \delta(E - E_n)$.

C. Harmonic inversion of band-limited signals

In this section we wish to solve the nonlinear set of equations

$$c_n = \sum_{k=1}^{K} d_k z_k^n \ , \quad n = 0, 1, \ldots, 2K-1 \ , \tag{11}$$

where $z_k \equiv \exp\left(-\mathrm{i}w'_k\tau\right)$ and d_k are, generally complex, variational parameters. For notational simplicity we have absorbed the factor of $-\mathrm{i}$ on the right-hand side of Eq. (10) into the d_k's with the understanding that this should be corrected for at the end of the calculation. We assume that the number of frequencies in the signal is relatively small ($K \sim 50$ to 200). Although the system of nonlinear equations is, in general, still ill-conditioned, frequency filtering reduces the number of signal points, and hence the number of equations. Several numerical techniques, that otherwise would be numerically unstable, can now be applied successfully. In the following we employ three different methods, viz. linear predictor (LP), Padé approximant (PA), and signal diagonalization (SD).

1. Linear Predictor

The problem of solving Eq. (11) has already been addressed in the 18th century by Baron de Prony [27], who converted the nonlinear set of equations (11) to a linear algebra problem. Today this method is known as linear predictor (LP). Our method strictly applies the procedure of LP except with one essential difference; the original signal $C^{\rm sc}(s)$ is replaced with its band-limited counterpart $c_n \equiv C^{\rm sc}_{\rm bl}(n\tau)$.

Equation (11) can be written in matrix form for the signal points c_{n+1} to c_{n+K},

$$\begin{pmatrix} c_{n+1} \\ \vdots \\ c_{n+K} \end{pmatrix} = \begin{pmatrix} z_1^{n+1} & \cdots & z_K^{n+1} \\ \vdots & \ddots & \vdots \\ z_1^{n+K} & \cdots & z_K^{n+K} \end{pmatrix} \begin{pmatrix} d_1 \\ \vdots \\ d_K \end{pmatrix} . \tag{12}$$

From the matrix representation (12) it follows that

$$c_n = (z_1^n \cdots z_K^n) \begin{pmatrix} z_1^{n+1} & \cdots & z_K^{n+1} \\ \vdots & \ddots & \vdots \\ z_1^{n+K} & \cdots & z_K^{n+K} \end{pmatrix}^{-1} \begin{pmatrix} c_{n+1} \\ \vdots \\ c_{n+K} \end{pmatrix} = \sum_{k=1}^{K} a_k c_{n+k} \ , \tag{13}$$

which means that every signal point c_n can be "predicted" by a linear combination of the K subsequent points with a fixed set of coefficients a_k, $k = 1, \ldots, K$. The first step of the LP method is to calculate these coefficients. Writing Eq. (13) in matrix form with $n = 0, \ldots, K-1$, we obtain the coefficients a_k as the solution of the linear set of equations,

$$\begin{pmatrix} c_1 & \cdots & c_K \\ \vdots & \ddots & \vdots \\ c_K & \cdots & c_{2K-1} \end{pmatrix} \begin{pmatrix} a_1 \\ \vdots \\ a_K \end{pmatrix} = \begin{pmatrix} c_0 \\ \vdots \\ c_{K-1} \end{pmatrix} . \tag{14}$$

The second step consists in determining the parameters z_k in Eq. (11). Using Eqs. (13) and (11) we obtain

$$c_n = \sum_{k=1}^{K} a_k c_{n+k} = \sum_{l=1}^{K} \sum_{k=1}^{K} a_k d_l z_l^{n+k} \ , \tag{15}$$

and thus

$$\sum_{k=1}^{K} \left[\sum_{l=1}^{K} a_l z_k^{n+l} - z_k^n \right] d_k = 0 \ . \tag{16}$$

Equation (16) is satisfied for arbitrary sets of amplitudes d_k when z_k is a zero of the polynomial

$$\sum_{l=1}^{K} a_l z^l - 1 = 0 \ . \tag{17}$$

The parameters $z_k = \exp(-{\rm i}w'_k\tau)$ and thus the frequencies

$$w_k' = \frac{\mathrm{i}}{\tau}\log(z_k) \tag{18}$$

are therefore obtained by searching for the zeros of the polynomial in Eq. (17). Note that this is the only nonlinear step of the algorithm, and numerical routines for finding the roots of polynomials are well established. In the third and final step, the amplitudes d_k are obtained from the linear set of equations

$$c_n = \sum_{k=1}^{K} d_k z_k^n \ , \quad n = 0, \ldots, K-1 \ . \tag{19}$$

To summarize, the LP method reduces the *nonlinear* set of equations (11) for the variational parameters $\{z_k, d_k\}$ to two well-known problems, i.e., the solution of two *linear* sets of equations (14) and (19) and the root search of a polynomial, Eq. (17), which is a nonlinear but familiar problem. The matrices in Eqs. (14) and (19) are a Toeplitz and Vandermonde matrix, respectively, and special algorithms are known for the fast solution of such linear systems [28]. However, when the matrices are ill-conditioned, conventional *LU* decomposition of the matrices is numerically more stable, and, furthermore, an iterative improvement of the solution can significantly reduce errors arising from numerical rounding. The roots of polynomials can be found, in principle, by application of Laguerre's method [28]. However, it turns out that an alternative method, i.e., the diagonalization of the Hessenberg matrix

$$\mathbf{A} = \begin{pmatrix} -\frac{a_{K-1}}{a_K} & -\frac{a_{K-2}}{a_K} & \cdots & -\frac{a_1}{a_K} & -\frac{a_0}{a_K} \\ 1 & 0 & \cdots & 0 & 0 \\ 0 & 1 & \cdots & 0 & 0 \\ \vdots & \vdots & \ddots & \vdots & \vdots \\ 0 & 0 & \cdots & 1 & 0 \end{pmatrix} \ , \tag{20}$$

for which the characteristic polynomial $P(z) = \det[\mathbf{A} - z\mathbf{I}] = 0$ is given by Eq. (17) (with $a_0 = -1$), is a numerically more robust technique for finding the roots of high degree ($K \gtrsim 60$) polynomials [28].

2. Padé Approximant

As an alternative method for solving the nonlinear system (11) we now propose to apply the method of Padé approximants (PA) to our band-limited signal c_n. Let us assume for the moment that the signal points c_n are known up to infinity, $n = 0, 1, \ldots \infty$. Interpreting the c_n's as the coefficients of a Maclaurin series in the variable z^{-1}, we can then define the function $g(z) = \sum_{n=0}^{\infty} c_n z^{-n}$. With Eq. (11) and the sum rule for geometric series we obtain

$$g(z) \equiv \sum_{n=0}^{\infty} c_n z^{-n} = \sum_{k=1}^{K} d_k \sum_{n=0}^{\infty} (z_k/z)^n = \sum_{k=1}^{K} \frac{z d_k}{z - z_k} \equiv \frac{P_K(z)}{Q_K(z)} \ . \tag{21}$$

The right-hand side of Eq. (21) is a rational function with polynomials of degree K in the numerator and denominator. Evidently, the parameters $z_k = \exp(-\mathrm{i}w_k'\tau)$ are the poles of $g(z)$, i.e., the zeros of the polynomial $Q_K(z)$. The parameters d_k are calculated via the residues of the last two terms of (21). We obtain

$$d_k = \frac{P_K(z_k)}{z_k Q'_K(z_k)} \ , \tag{22}$$

with the prime indicating the derivative d/dz. Of course, the assumption that the coefficients c_n are known up to infinity is not fulfilled and, therefore, the sum on the left-hand side of Eq. (21) cannot be evaluated in practice. However, the convergence of the sum can be accelerated by application of PA. Indeed, with PA, knowledge of $2K$ signal points $c_0, \ldots, c_{2K-1}$ is sufficient for the calculation of the coefficients of the two polynomials

$$P_K(z) = \sum_{k=1}^{K} b_k z^k \quad \text{and} \quad Q_K(z) = \sum_{k=1}^{K} a_k z^k - 1 \ . \tag{23}$$

The coefficients a_k, $k = 1, \ldots, K$ are obtained as solutions of the linear set of equations

$$c_n = \sum_{k=1}^{K} a_k c_{n+k} \ , \quad n = 0, \ldots, K-1 \ ,$$

which is identical to Eqs. (13) and (14) for LP. Once the a's are known, the coefficients b_k are given by the *explicit* formula

$$b_k = \sum_{m=0}^{K-k} a_{k+m} c_m \ , \quad k = 1, \ldots, K \ . \tag{24}$$

It should be noted that the different derivations of LP and PA yield the same polynomial whose zeros are the z_k parameters, i.e., the z_k calculated with both methods exactly agree. However, LP and PA do differ in the way the amplitudes, d_k, are calculated. It is also important to note that PA is applied here as a method for signal processing, i.e., in a different context to that in Sec. III, where the Padé approximant is used for the direct summation of the periodic orbit terms in semiclassical trace formulae.

3. Signal Diagonalization

In Refs. [14,16] it has been shown how the problem of solving the nonlinear set of equations (11) can be recast in the form of the generalized eigenvalue problem,

$$\mathbf{U}\boldsymbol{B}_k = z_k \mathbf{S}\boldsymbol{B}_k \ . \tag{25}$$

The elements of the $K \times K$ operator matrix $\mathbf{U}$ and overlap matrix $\mathbf{S}$ depend trivially upon the c_n's [16]:

$$U_{ij} = c_{i+j+1} \ ; \quad S_{ij} = c_{i+j} \ ; \quad i, j = 0, \ldots, K-1 \ . \tag{26}$$

Note that the operator matrix $\mathbf{U}$ is the same as in the linear system (14), i.e., the matrix form of Eq. (13) of LP. The matrices $\mathbf{U}$ and $\mathbf{S}$ in Eq. (25) are complex symmetric (i.e., non-Hermitian), and the eigenvectors $\boldsymbol{B}_k$ are orthogonal with respect to the overlap matrix $\mathbf{S}$,

$$(\boldsymbol{B}_k | \mathbf{S} | \boldsymbol{B}_{k'}) = N_k \delta_{kk'} \ , \tag{27}$$

where the brackets define a complex symmetric inner product $(a|b) = (b|a)$, i.e., no complex conjugation of either a or b. The overlap matrix $\mathbf{S}$ is not usually positive definite and therefore the N_k's are, in general complex, normalization parameters. An eigenvector $\boldsymbol{B}_k$ cannot be normalized for $N_k = 0$. The amplitudes d_k in Eq. (11) are obtained from the eigenvectors $\boldsymbol{B}_k$ via

$$d_k = \frac{1}{N_k} \left[\sum_{n=0}^{K-1} c_n \boldsymbol{B}_{k,n} \right]^2 . \tag{28}$$

The parameters z_k in Eq. (11) are given as the eigenvalues of the generalized eigenvalue problem (25), and are simply related to the frequencies w'_k in Eq. (10) via $z_k = \exp(-\mathrm{i}w'_k\tau)$.

The three methods introduced above (LP, PA and SD) look technically quite different. With LP the coefficients of the characteristic polynomial (17) and the amplitudes d_k are obtained by solving two linear sets of equations (14) and (19). Note that the complete set of zeros z_k of Eq. (17) is required to solve for the d_k in Eq. (19). The PA method is even simpler, as only one linear system, Eq. (14), has to be solved to determine the coefficients of the rational function $P_K(z)/Q_K(z)$. Finding the zeros of Eq. (17) provides knowledge about selected parameters z_k, and allows one to calculate the corresponding amplitudes d_k via Eq. (22). The SD method requires the most numerical effort, because the solution of the generalized eigenvalue problem (25) for both the eigenvalues z_k and eigenvectors $\boldsymbol{B}_k$ is needed.

It is important to note that the three techniques, in spite of their different derivations, are mathematically equivalent and provide the same results for the parameters $\{z_k, d_k\}$, when the following two conditions are fulfilled: the nonlinear set of equations (11) has a unique solution, when, firstly, the matrices $\mathbf{U}$ and $\mathbf{S}$ in Eq. (26) have a non-vanishing determinant ($\det \mathbf{U} \neq 0$, $\det \mathbf{S} \neq 0$), and, secondly, the parameters z_k are non-degenerate ($z_k \neq z_{k'}$ for $k \neq k'$). These conditions guarantee the existence of a unique solution of the linear equations (14) and (19), the non-singularity of the generalized eigenvalue problem (25), and the non-vanishing of both the derivatives $Q'_K(z_k)$ in Eq. (22) and the normalization constants N_k in Eqs. (27) and (28). Equation (11) usually has no solution in the case of degenerate z_k parameters, however, degeneracies can be handled with a generalization of the ansatz (11) and modified equations for the calculation of the parameters. Here, we will not further discuss this special case.

While the parameters z_k in Eq. (11) are usually unique, the calculation of the frequencies w'_k via Eq. (18) is not unique, because of the multivalued property of the complex logarithm. To obtain the "correct" frequencies it is necessary to appropriately adjust the range Δw of the frequency filter and the step width τ of the band-limited signal (10). From our numerical experience we recommend the following procedure. The most convenient approach is to choose first the center w_0 of the frequency window and the number K of frequencies within that window. Note that K determines the dimension of the linear systems, and hence the degree of the polynomials which have to be handled numerically, and is therefore directly related to the computational effort required. Frequency windows are selected to be sufficiently narrow to yield values for the rank between $K \approx 50$ and $K \approx 200$. The step width for the band-limited signal should be chosen as

$$\tau = \frac{s_{\max}}{2K} , \tag{29}$$

with $s_{\max}$ being the total length of the periodic orbit signal. The relation $z_k = \exp(-\mathrm{i}w'_k\tau)$ projects the frequency window $w' \in [-\Delta w, +\Delta w]$ onto the unit circle in the complex plane when the range of the frequency window is chosen as

$$\Delta w = \frac{\pi}{\tau} = \frac{2\pi K}{s_{\max}} \; . \tag{30}$$

When calculating the complex logarithm with $\arg\log z \in [-\pi, +\pi]$, Eq. (18) provides the "correct" shifted frequencies w'_k and thus the frequencies $w_k = w_0 + w'_k$.

To achieve convergence, the length $s_{\max}$ of the periodic orbit signal must be sufficiently long to ensure that the number of semiclassical eigenvalues within the frequency window is less than K. As a consequence the harmonic inversion procedure usually provides not only the true semiclassical eigenvalues but also some spurious resonances. The spurious resonances are identified by low or near zero values of the corresponding amplitudes d_k and can also be detected by analyzing the shifted band-limited signal, i.e., signal points $c_1, \ldots, c_{2K}$ instead of $c_0, \ldots, c_{2K-1}$. The true frequencies usually agree to very high precision, while spurious frequencies show by orders of magnitude larger deviations.

The harmonic inversion method introduced above will be applied in Sec. IV A to the periodic orbit quantization of the three-disk scattering system, and the semiclassical resonances will be compared with results obtained by the cycle-expansion technique [4,29,30] and the direct application of the Padé approximant to periodic orbit sums discussed in the next Section III.

III. SEMICLASSICAL QUANTIZATION BY PADÉ APPROXIMANTS TO PERIODIC ORBIT SUMS

The method presented in the previous Section is based on signal processing (harmonic inversion) of the periodic orbit signal. In this Section we introduce our second method for semiclassical quantization, based on the direct application of the Padé approximant to periodic orbit sums.

The PA to a complex function $f(z)$ is defined as a ratio of two polynomials and can be computed from the coefficients a_n of the Maclaurin expansion of $f(z)$, i.e., a power series

$$f(z) = \sum_{n=0}^{\infty} a_n z^n$$

with finite or even zero radius of convergence in z [20]. However, Eq. (1) does not have the functional form of a Maclaurin power series expansion of $g(E)$ in the energy E. Even disregarding this limitation, a direct computation of the PA to the sum in Eq. (1) would be numerically unstable due to the typically large number of periodic orbit terms. Nevertheless, considering E as a parameter, $g(E)$ can be rearranged and written as a formal power series in an auxiliary variable z,

$$g(z;E) = \sum_n \sum_{\mu_{\rm po}=n} \mathcal{A}_{\rm po}(E) \mathrm{e}^{\mathrm{i}S_{\rm po}(E)/\hbar} z^n \;\equiv\; \sum_n a_n(E) z^n \; , \tag{31}$$

where the maximum value of n required for convergence of the PA is relatively small compared with the number of periodic orbit terms. Of course, the arrangement (31) of the

periodic orbit sum as a power series is not unique, and expansions similar to Eq. (31) can be used for other ordering parameters n of the orbits, e.g., the cycle length in systems with a symbolic code. However, if no symbolic dynamics exists, the sorting of orbits by their Maslov index is natural both physically and as a way to introduce an integer summation index and will be justified in Sec. IV by the successful numerical application of the method to a regular system without symbolic dynamics. Note that the PA to the periodic orbit sum cannot be applied without any ordering parameter, i.e., when no symbolic dynamics exists and all Maslov indices are zero, which is the case, e.g., for the Riemann zeta function as a mathematical model for periodic orbit quantization [9]. The true value $g(E)$ of the periodic orbit sum is obtained by setting $z = 1$ in Eq. (31), i.e., $g(E) = g(1; E)$. In such a case, we have a point PA which is given as a ratio of two polynomials in z whose coefficients are non-polynomial functions of E all at a fixed value of z. The usual implementation of the PA as a ratio of two polynomials in z whose coefficients are computed, e.g., via the Longman algorithm [31] would be advantageous if $g(z; E)$ were required for many values of z. In the present case, at each given energy E only one fixed value $z = 1$ is needed and the PA is most efficiently computed by means of the recursive Wynn ε-algorithm [32].

To briefly describe the ε-algorithm, we introduce a sequence of partial sums $\{A_n\}$ which converges to (or diverges from) its limit A as $n \to \infty$. In the case of divergence, A is called the 'anti-limit' of $\{A_n\}$, as $n \to \infty$. Further, let F be a transformation which maps $\{A_n\}$ into another sequence $\{B_n\}$. The mapping F will represent an accelerator, i.e., the sequence $\{B_n\}$ will converge to the same limit A faster than $\{A_n\}$ if the condition

$$\frac{B_n - B}{A_n - A} \to 0$$

is fulfilled as $n \to \infty$. In addition, the same F can be applied to wildly divergent sequences $\{A_n\}$. Only nonlinear mappings can simultaneously accomplish both goals to accelerate slowly convergent and induce convergence into divergent sequences. The transformation F will be nonlinear if its coefficients depend on A_n, e.g., the so-called e-algorithm of Shanks [33], whose mapping F is the operator e_k which converts the sequence $\{A_n\}$ into $\{B_n\}$ via

$$e_k(A_n) = B_{k,n} = [n + k/k] \tag{32}$$

with $n \geq 0$ and $n \geq k$. This is the well-known Aitken Δ^2-iteration process (i.e., the simplest PA, [1/1]) extended to higher orders k. The general term in the kth-order transform $B_{k,n}$ of A_n can be computed efficiently from the stable and recursive ε-algorithm of Wynn [32], viz.,

$$e_s(A_m) = \varepsilon_{2s}^{(m)} = [m + s/s] \,, \tag{33}$$

where

$$\varepsilon_{s+1}^{(m)} = \varepsilon_{s-1}^{(m+1)} + \frac{1}{\varepsilon_s^{(m+1)} - \varepsilon_s^{(m)}} \quad ; \quad m, s \geq 0 \tag{34}$$

with $\varepsilon_{-1}^{(m)} = 0$, $\varepsilon_0^{(m)} = A_m$, $\varepsilon_{2s+1}^{(m)} = 1/e_s(\Delta A_m)$, and where Δ is the forward difference operator: $\Delta x_j = x_{j+1} - x_j$. When $\{A_n\}$ is the sequence of partial sums of a power series,

the two-dimensional array $\varepsilon_{2s}^{(m-s)}$ yields the upper half of the well known Padé table $[m/s]$. However, the ε-algorithm need not necessarily be limited to power series.

The procedure to apply the above PA to semiclassical quantization by summation of periodic orbit terms works as follows. For a given system we calculate the periodic orbits up to a chosen maximum ordering parameter $n \leq n_{\max}$, where n can be but is not necessarily related to the Maslov indices of orbits. Note that this set of orbits usually differs from the set of orbits with classical action $S_{\rm po} \leq S_{\max}$, which is required for periodic orbit quantization by harmonic inversion in Sec. II. From the periodic orbit amplitudes $\mathcal{A}_{\rm po}$ (including the phases $\exp(-\mathrm{i}\frac{\pi}{2}\mu_{\rm po})$ given by the Maslov indices) and actions $S_{\rm po}$, we compute the partial sums (e.g., with $n \leq \mu_{\max}$ the Maslov index):

$$A_n = \sum_{\mu_{\rm po} \leq n} \mathcal{A}_{\rm po}(E) \mathrm{e}^{\mathrm{i}S_{\rm po}(E)/\hbar} \ . \tag{35}$$

The sequence $\{A_n\}$ of partial sums is used as input to the ε-algorithm, Eq. (34), to obtain a converged value $g(E)$ of the periodic orbit sum (1). The semiclassical eigenenergies or resonances are given as the poles of $g(E)$ and are obtained by searching numerically for the zeros of the reciprocal function $1/g(E)$. Such a search requires the evaluation of, e.g., $\mathcal{A}_{\rm po}(E)$ and $S_{\rm po}(E)$, at complex values of E. This can be done in a straightforward manner for the scaling systems considered in this paper. The number of the poles of $g(E)$ is not constrained by the size of the sequence $\{A_n\}$ of partial sums since our PA is a ratio of two non-polynomial functions of E.

It is important to note that the Padé approximant is applied here in a completely different context than in the first method where it is used as a tool for signal processing. In Sec. II we have shown that the three techniques LP, PA and SD used for the harmonic inversion of band-limited signals are mathematically equivalent. However, the two methods for periodic orbit quantization introduced in Sections II and III are not necessarily equivalent, and it may well be that one or the other method is more appropriate for the semiclassical quantization of a given physical system. Numerical results for two physical systems with completely different dynamical properties will be presented in the next Sec. IV.

IV. RESULTS AND DISCUSSION

In this section we want to demonstrate the efficiency and accuracy of the methods introduced above by way of two examples: the three-disk repeller as an open physical system with classically chaotic dynamics and the circle billiard as a bound regular system. Both systems have previously been investigated by means of FD [8,9,12,34–36]. The three-disk repeller has also served as a prototype for the development and application of cycle expansion techniques [4,29,30], and for this system we will compare the convergence properties of three different methods, viz. harmonic inversion, Padé approximant and cycle expansion.

A. The three-disk repeller

As the first example we consider a billiard system consisting of three identical hard disks with radius R, displaced from each other by the same distance d. This simple, albeit

nontrivial, scattering system has served as a model for the development of the cycle expansion method [4,21,29,30] and periodic orbit quantization by harmonic inversion [8,9,12]. The three-disk scattering system is invariant under the symmetry operations of the group C_{3v}, *i.e.*, three reflections at symmetry lines and two rotations by $2\pi/3$ and $4\pi/3$. Resonances belong to one of the three irreducible subspaces A_1, A_2, and E [37]. As in most previous work we concentrate on the resonances of the subspace A_1 for the three-disk repeller with $R = 1$ and $d = 6$. In billiards, which are scaling systems, the shape of periodic orbits does not depend on the energy E, and the classical action is given by the length L of the orbit ($S_{\rm po} = \hbar k L_{\rm po}$), where $k = |\mathbf{k}| = \sqrt{2ME}/\hbar$ is the absolute value of the wave vector to be quantized. We have calculated all periodic orbits with Maslov index $\mu_{\rm po} \leq 30$, which corresponds to the set of orbits with cycle length $n \leq 15$.

1. Harmonic inversion of the periodic orbit signal

We first calculate the semiclassical resonances of the three-disk repeller by the method introduced in Sec. II, viz. harmonic inversion of the periodic orbit signal [see Eq. (4)]

$$C^{\rm sc}(L) = \sum_{\rm po} \mathcal{A}_{\rm po} \delta(L - L_{\rm po}) \ .$$

[Setting $\hbar = 1$, we use $s = L$ in what follows.] In Fig. 1a we present the periodic orbit signal $C^{\rm sc}(L)$ for the three-disk repeller in the region $0 \leq L \leq L_{\rm max} = 35$. The signal is given as a periodic orbit sum of delta functions $\delta(L - L_{\rm po})$ weighted with the periodic orbit amplitudes $\mathcal{A}_{\rm po}$. The groups with oscillating sign belong to periodic orbits with adjacent cycle lengths. Signals of this type have been analyzed (after convolution with a narrow Gaussian function, see Eq. (7)) by FD in Refs. [8–12]. We now illustrate the harmonic inversion of band-limited periodic orbit signals by LP, PA and SD.

In a first step, a band-limited periodic orbit signal is constructed as described in Sec. II B. As an example we choose $K = 100$ as the rank of the nonlinear set of equations (10), and $k_0 = 200$ as the center of the frequency window. The width of the frequency window is given by $\Delta k = 2\pi K/L_{\rm max} = 200\pi/35 \approx 18.0$. The step width of the band-limited signal is $\tau = \Delta L = L_{\rm max}/2K = 0.175$. The signal points $c_n = C^{\rm sc}_{\rm bl}(L = n\Delta L)$, with $n = 0, \ldots, 2K$ are calculated with the help of Eq. (8) and presented in Fig. 1b. The solid and dashed lines are the real and imaginary parts of $C^{\rm sc}_{\rm bl}(n\Delta L)$, respectively. The modulations with spacings $\pi/\Delta k$ result from the superposition of the sinc-like functions in Eq. (8).

The band-limited periodic orbit signal $C^{\rm sc}_{\rm bl}(n\Delta L)$ can now be analyzed, in a second step, with one of the harmonic inversion techniques introduced in Sec. II C, viz. LP, PA or SD. The resonances obtained by LP are presented as plus symbols in Fig. 1c. The dotted lines at Re $k = 182$ and Re $k = 218$ show the borders of the frequency window. The two symbols very close to the border on the left indicate spurious resonances.

A long range spectrum can be obtained by choosing several values w_0 for the center of the frequency window in such a way that the windows slightly overlap. By analyzing a periodic orbit signal similar to that in Fig. 1b but with an increased signal length, $L_{\rm max} = 55$ we have calculated the semiclassical resonances of the three-disk repeller in the range $0 \leq$ Re $k \leq 250$. It turns out that they are even more accurate than those obtained previously [9,12] using FD. For more details see Ref. [13]. Part of the resonances in the range $25 \leq$ Re $k \leq 65$ are

marked as squares in Fig. 2. The comparison of resonances in Fig. 2 obtained by various semiclassical quantization methods will be discussed below.

2. Padé approximant to the periodic orbit sum

We now apply our second method introduced in Sec. III, the PA to the periodic orbit sum to the same system as discussed above, viz. the three-disk repeller with $R = 1$ and $d = 6$. We have calculated the partial sums $\{A_n\}$ of periodic orbit terms (see Eq. 35) using all periodic orbits with cycle length $n \leq 15$, which corresponds to the set of orbits with Maslov index $\mu_{\rm po} \leq 30$. The sequence of the partial sums $\{A_n\}$ of periodic orbit terms in Eq. (35) converges for wave numbers k above the borderline Im $k = -0.121\,557$ [4] which separates the domain of absolute convergence of the periodic orbit sum from the domain where analytic continuation is necessary, but strongly diverges deep in the complex plane, where the resonance poles are located. This is illustrated in Fig. 3 for two different wave numbers k. The dashed line and the plus symbols in Fig. 3a show the convergence of the sequence $\{A_n\}$ at $k = 150 - 0.1$i. What is plotted is the absolute value of the difference between two consecutive terms, $\varepsilon = |A_n - A_{n-1}|$. As can be seen this sequence is slowly convergent, and about two to three significant digits are obtained at $n = 15$. The convergence can be accelerated using the PA, as is seen by the solid line and squares in Fig. 3a showing the error values $\varepsilon = |A_n^{\rm PA} - A_{n-1}^{\rm PA}|$ for the sequence of the Padé approximants $\{A_n^{\rm PA}\}$ to the periodic orbit sum. The periodic orbit sum has converged to six significant digits already for $n = 10$. The situation is even much more dramatic in the deep complex plane (Im $k < -0.122$), *e.g.*, at $k = 150 - 0.5$i. Here, the sequence of the partial sums $\{A_n\}$ of periodic orbit terms exhibits *exponential* divergence, as can be seen from the dashed line and plus symbols in Fig. 3b. Nevertheless, this sequence converges when subjected to the PA implemented through the ε-algorithm (solid line and squares in Fig. 3b).

The resonances of the three-disk scattering systems have been obtained by a numerical two-dimensional root search in the complex k-plane for the zeros of the function $1/g(k)$, where $g(k)$ is the PA to the periodic orbit sum. The subset of the semiclassical resonances in the range $25 \leq$ Re $k \leq 65$ are marked by the plus symbols in Fig. 2. They agree well with the squares obtained by harmonic inversion of the periodic orbit signal. For the resonances shown in Fig. 2 we will now discuss the applicability and limitations of the different semiclassical methods to some more extent.

3. Harmonic inversion and Padé approximant vs. cycle expansion

The three-disk scattering system discussed above has purely hyperbolic classical dynamics and has been used extensively as the prototype model for the cycle expansion techniques [4,21,29,30]. As has been shown by Voros [38], Gutzwiller's trace formula for unstable periodic orbits can be recast in the form of an infinite and non-convergent Euler product over all periodic orbits. When the periodic orbits obey a symbolic dynamics the semiclassical eigenenergies or resonances can be obtained as the zeros of the cycle expanded Gutzwiller-Voros zeta function. Unfortunately, the convergence of the cycle expansion is restricted, due to poles of the Gutzwiller-Voros zeta function [21]. The domain of analyticity of semiclassical

zeta functions can be extended [39,40] resulting in the "quasiclassical zeta function" [40,30], which is an entire function for the three-disk repeller. This approach allows one to calculate semiclassical resonances in critical regions where the Gutzwiller-Voros zeta function does not converge, at the cost, however, of many extra spurious resonances and with the rate of convergence being slowed down tremendously [30].

It is very interesting and illustrative to compare the convergence properties of the various methods which have been applied for periodic orbit quantization of the three-disk repeller, viz. the two methods introduced in Sections II and III of this paper and the cycle expansion technique. We will demonstrate that the harmonic inversion method and the PA to periodic orbit sums provide semiclassical resonances in energy regions where the cycle expansion of the Gutzwiller-Voros zeta function does not converge. With the limited numerical accuracy of harmonic inversion by FD applied in Ref. [9], the semiclassical resonances of the three-disk repeller in the region Im $k < -0.6$ were somewhat unreliable. The analysis of band-limited periodic orbit signals introduced in the present paper now allows us to calculate semiclassical resonances of much improved accuracy even deep in the complex plane.

Fig. 2 presents the results of the three different methods in the region $25 \leq \mathrm{Re}\ k \leq 65$. The resonances calculated by harmonic inversion and the PA to periodic orbit sum are marked by the squares and plus symbols as already mentioned above. The crosses label the resonances obtained by the cycle expansion of the Gutzwiller-Voros zeta function [30]. The dotted line in Fig. 2 indicates the borderline, Im $k = -0.121\,557$ [4], which separates the domain of absolute convergence of Gutzwiller's trace formula from the region where analytic continuation is necessary. For the two resonance bands slightly below this border the results of all three semiclassical quantization methods are in perfect agreement. The dashed line in Fig. 2 marks the borderline of absolute convergence of the Gutzwiller-Voros zeta function, at Im $k = -0.699\,110$ [39]. The Gutzwiller-Voros zeta function provides several spurious resonances which accumulate at Im $k \approx -0.9$, i.e., slightly below the borderline of absolute convergence (see the crosses in Fig. 2). The resonances in the region Im $k < -0.9$, especially those belonging to the fourth band, are not described by the Gutzwiller-Voros zeta function but are obtained by both the harmonic inversion method and the Padé approximant to the periodic orbit sum (see the squares and plus symbols in Fig. 2, respectively).

B. The circle billiard

As the second example we now demonstrate the applicability of our semiclassical quantization methods to the circle billiard. This system has previously been investigated as a model for periodic orbit quantization of integrable systems [41,42], however, to the best of our knowledge, has not yet been treated by the cycle expansion technique [4] or pseudo-orbit expansion [5].

The exact quantum mechanical eigenvalues $E = \hbar^2 k^2/2M$ of the circle billiard are given by zeros of Bessel functions $J_{|m|}(kR) = 0$, where $m = 0, \pm 1, \pm 2, , \ldots$ is the angular momentum quantum number and R is the radius of the circle. The semiclassical eigenvalues can be obtained by an Einstein-Brillouin-Keller (EBK) torus quantization [43] resulting in the quantization condition

$$kR\sqrt{1-(m/kR)^2} - |m| \arccos \frac{|m|}{kR} = \pi \left(n + \frac{3}{4}\right) \tag{36}$$

where $n = 0, 1, 2, \ldots$ is the radial quantum number. In the following we choose $R = 1$. States with angular momentum quantum number $m \neq 0$ are twofold degenerate.

The periodic orbits of the circle billiard have the form of regular polygons. They can be labeled by two integer numbers m_r and m_φ with the restriction $m_r \geq 2m_\varphi$ which can be shown to be identical with the number of sides of the corresponding polygon and its number of turns around the center of the circle, respectively [41]. Some examples are given in Fig. 4. The angle between two bounces is a rational multiple of 2π, i.e., the periods $L_{\rm po}$ are obtained from the condition

$$L_{\rm po} = 2m_r \sin\gamma \ , \tag{37}$$

with $\gamma \equiv \pi m_\phi / m_r$. Periodic orbits with $m_r \neq 2m_\phi$ can be traversed in two directions and thus have multiplicity 2. For the amplitudes $\mathcal{A}_{\rm po}$ of the circle billiard, the Berry-Tabor formula [3] for integrable systems yields

$$\mathcal{A}_{\rm po} = \sqrt{\frac{\pi}{2}} \frac{L_{\rm po}^{3/2}}{m_r^2} \, \mathrm{e}^{-\mathrm{i}\frac{\pi}{2}\left(3m_r + \frac{1}{2}\right)} \ , \tag{38}$$

with $\mu_{\rm po} = 3m_r$ being the Maslov index.

The periodic orbit quantities can be used to set up the semiclassical recurrence signal (4) for the circle billiard which can then be analyzed by harmonic inversion to extract the eigenenergies. Detailed comparisons between results obtained by harmonic inversion and the EBK torus quantization (36) are presented in Refs. [12,34–36] and show excellent agreement. The harmonic inversion method can even be generalized, firstly, to the harmonic inversion of cross-correlated periodic orbit sums [35,44] which allows to significantly reduce the number of orbits required for semiclassical quantization, and, secondly, to include higher order $\hbar$ corrections in the periodic orbit sum. We do not report these results here but refer the reader to the literature for details. In what follows we want to apply our second method introduced in Sec. III to the circle billiard.

It follows from Eq. (38) that the Padé approximant to the periodic orbit sum should be calculated with an ordering parameter $n = m_r - 1$, i.e.,

$$A_n(k) = \sum_{m_r < n} \mathcal{A}_{\rm po} \mathrm{e}^{\mathrm{i}kL_{\rm po}} \ , \quad n = 1, 2, \ldots \ , \tag{39}$$

with the lengths $L_{\rm po}$ and amplitudes $\mathcal{A}_{\rm po}$ given by Eqs. (37) and (38), respectively. We included all periodic orbits (m_r, m_φ) with $m_r < 100$ in the calculation of the function $g(k)$ which is the Padé approximant to the sequence $A_n(k)$. The real and imaginary parts of $1/g(k)$ are presented as solid and dashed lines respectively in Fig. 5. The zeros of the function $1/g(k)$ agree perfectly to at least seven significant digits with the exact positions of the semiclassical eigenvalues obtained from Eq. (36) and marked by the squares in Fig. 5.

V. CONCLUSION

We have introduced two different methods to make semiclassical periodic orbit sums convergent. The first method is based on the harmonic inversion of band-limited periodic orbit signals. The characteristic feature of this method is the strict separation of the two steps,

viz. firstly, the analytical filtering of the periodic orbit signal and, secondly, the numerical harmonic inversion of the band-limited signal by application of either linear predictor (LP), Padé approximant (PA), or signal diagonalization (SD). The separation of these two steps and the handling of small amounts of data compared to other "black box" type signal processing techniques provides a transparent approach to harmonic inversion as a semiclassical quantization method thus opening the possibility to an easier and deeper understanding of semiclassical quantization itself, and even yields numerically more accurate results than previous applications of filter-diagonalization (FD). The harmonic inversion method can be applied to the periodic orbit quantization of systems with both chaotic and regular classical dynamics, when the periodic orbit signal is calculated with Gutzwiller's trace formula [1,2] for isolated orbits and the Berry-Tabor formula [3] for orbits on rational tori, respectively. More generally, any signal given as a sum of δ functions can be filtered analytically and analyzed using the methods described in Sections II B and II C. For example, the technique can also be applied to the harmonic inversion of the density of states $\varrho(E) = \sum_n \delta(E - E_n)$ of quantum spectra to extract information about the underlying classical dynamics [12,25,26].

The second method is the direct application of the Padé approximant (PA) to periodic orbit sums, and allows the resummation of the typically exponentially divergent terms of the semiclassical trace formulae. The Padé approximant can be applied when the total periodic orbit sum can be divided into partial sums with respect to an integer ordering parameter n, which can be related to, e.g., the cycle length of a symbolic code or the Maslov index of the orbit.

The two methods for periodic orbit quantization have been demonstrated for systems with completely different classical dynamics, viz. the classically chaotic three-disk scattering problem and the integrable circle billiard. A detailed comparison of various semiclassical quantization methods for the three-disk repeller reveals that quantization by harmonic inversion and the Padé approximant to periodic orbit sums can even be applied in energy regions where the cycle expansion of the Gutzwiller-Voros zeta function does not converge.

Evidently, the scope of applications of the methods presented in this paper is wide, and runs from simple models to challenging atomic, molecular, and mesoscopic systems with typically mixed regular-chaotic classical dynamics. Thus, even thirty years after the renaissance of semiclassics by Martin Gutzwiller, new and unexpected insights may be gained into the no man's land between classical and quantum physics.

ACKNOWLEDGMENTS

Fruitful discussions with Dž. Belkić, P. A. Dando, and H. S. Taylor are gratefully acknowledged. We thank A. Wirzba for supplying numerical data on the three-disk system. This work was supported in part by the Deutsche Forschungsgemeinschaft and Deutscher Akademischer Austauschdienst.

REFERENCES

[1] M. C. Gutzwiller, *J. Math. Phys.* **8**, 1979–2000 (1967); *J. Math. Phys.* **12**, 343–358 (1971).

[2] M. C. Gutzwiller, *Chaos in Classical and Quantum Mechanics* (Springer, New York, 1990).

[3] M. V. Berry and M. Tabor, *Proc. R. Soc. London* **A 349**, 101–123 (1976); *J. Phys. A* **10**, 371 (1977).

[4] P. Cvitanović P and B. Eckhardt, *Phys. Rev. Lett.* **63**, 823–826 (1989).

[5] M. V. Berry and J. P. Keating, *J. Phys. A* **23**, 4839–4849 (1990); *Proc. R. Soc. London* **A 437**, 151–173 (1992).

[6] E. B. Bogomolny, *Chaos* **2**, 5–13 (1992); *Nonlinearity* **5**, 805–866 (1992).

[7] R. Aurich, C. Matthies, M. Sieber, and F. Steiner, *Phys. Rev. Lett.* **68**, 1629–1632 (1992).

[8] J. Main, V. A. Mandelshtam, and H. S. Taylor, *Phys. Rev. Lett.* **79**, 825–828 (1997).

[9] J. Main, V. A. Mandelshtam, G. Wunner, and H. S. Taylor, *Nonlinearity* **11**, 1015–1035 (1998).

[10] J. Main and G. Wunner, *Phys. Rev. A* **59**, R2548–R2551 (1999).

[11] J. Main and G. Wunner, *Phys. Rev. Lett.* **82**, 3038–3041 (1999).

[12] J. Main, *Phys. Rep.* **316**, 233–338 (1999).

[13] J. Main, P. A. Dando, Dž. Belkić, and H. S. Taylor, *J. Phys. A* **33**, 1247–1263 (2000).

[14] M. R. Wall and D. Neuhauser, *J. Chem. Phys.* **102**, 8011–8022 (1995).

[15] V. A. Mandelshtam and H. S. Taylor, *Phys. Rev. Lett.* **78**, 3274–3277 (1997).

[16] V. A. Mandelshtam and H. S. Taylor, *J. Chem. Phys.* **107**, 6756–6769 (1997); **109**, 4128 (1998) (erratum).

[17] J. Main, P. A. Dando, Dž. Belkić, and H. S. Taylor, *Europhys. Lett.* **48**, 250–256 (1999).

[18] G. A. Baker, *Essentials of Padé Approximants* (Academic, New York, 1975).

[19] J. Čížek and E. R. Vrscay, *Int. J. Quantum Chem.* **21**, 27 (1982); H. J. Silverstone, B. G. Adams, J. Čížek, and P. Otto, *Phys. Rev. Lett.* **43**, 1498 (1979).

[20] Dž. Belkić, *J. Phys. A* **22**, 3003–3010 (1989).

[21] B. Eckhardt and G. Russberg, *Phys. Rev. E* **47**, 1578–1588 (1993).

[22] Dž. Belkić, P. A. Dando, J. Main, and H. S. Taylor, *J. Chem. Phys.* **113**, 6542–6556 (2000).

[23] S. D. Silverstein and M. D. Zoltowski, *Digital Signal Processing* **1**, 161–175 (1991).

[24] Dž. Belkić, P. A. Dando, H. S. Taylor, and J. Main, *Chem. Phys. Lett.* **315**, 135–139 (1999); Dž. Belkić, P. A. Dando, J. Main, H. S. Taylor, and S. K. Shin, *J. Phys. Chem. A*, in press.

[25] J. Main, V. A. Mandelshtam, and H. S. Taylor, *Phys. Rev. Lett.* **78**, 4351–4354 (1997).

[26] B. Grémaud and D. Delande, *Phys. Rev. A* **61**, 032504 (2000).

[27] Baron Gaspard Riche de Prony, *Essai expérimental et analytique: sur les lois de la dilatabilité de fluides élastique et sur celles de la force expansive de la vapeur de l'alkool, diffrentes températures*, Journal de l'École Polytechnique, volume 1, cahier 22, 22–76 (1795).

[28] W. H. Press, S. A. Teukolsky, W. T. Vetterling, and B. P. Flannery, *Numerical Recipes*, 2nd ed., (Cambridge University Press, Cambridge, 1992).

[29] B. Eckhardt, G. Russberg, P. Cvitanović, P. E. Rosenqvist, and P. Scherer, in *Quantum*

Chaos between Order and Disorder, G. Casati and B. V. Chirikov, eds. (Cambridge University Press, Cambridge, 1995), pp. 405–433.
[30] A. Wirzba, *Phys. Rep.* **309**, 1–116 (1999).
[31] I. M. Longman, *Int. J. Comp. Math. B* **3**, 53 (1971).
[32] P. Wynn, *Mathematical Tables and Other Aids for Computations* **10**, 91 (1956); *SIAM J. Numer. Anal.* **3**, 91 (1966); E. J. Weniger, *Comp. Phys. Rep.* **10**, 189–371 (1989).
[33] D. Shanks, *J. Math. Phys.* **34**, 1 (1955).
[34] J. Main, K. Weibert, and G. Wunner, *Phys. Rev. E* **58**, 4436–4439 (1998).
[35] J. Main and G. Wunner, *Phys. Rev. E* **60**, 1630–1638 (1999); J. Main, K. Weibert, V. A. Mandelshtam, and G. Wunner, *ibid*, 1639–1642 (1999).
[36] K. Weibert, J. Main, and G. Wunner, *Eur. Phys. J. D* **12**, 381–401 (2000).
[37] P. Cvitanović and B. Eckhardt, *Nonlinearity* **6**, 277–311 (1993).
[38] A. Voros, *J. Phys. A* **21**, 685–692 (1988).
[39] P. Cvitanović, P. E. Rosenqvist, G. Vattay, and H. H. Rugh, *Chaos* **3**, 619–636 (1993).
[40] P. Cvitanović and G. Vattay, *Phys. Rev. Lett.* **71**, 4138–4141 (1993).
[41] R. Balian and C. Bloch, *Ann. Phys.* **69**, 76–160 (1972).
[42] S. M. Reimann, M. Brack, A. G. Magner, J. Blaschke, and M. V. N. Murthy, *Phys. Rev. A* **53**, 39–48 (1996).
[43] I. C. Percival, *Adv. Chem. Phys.* **36**, 1–61 (1977).
[44] S. Hortikar and M. Srednicki, *Phys. Rev. E* **61**, R2180–R2183 (2000).

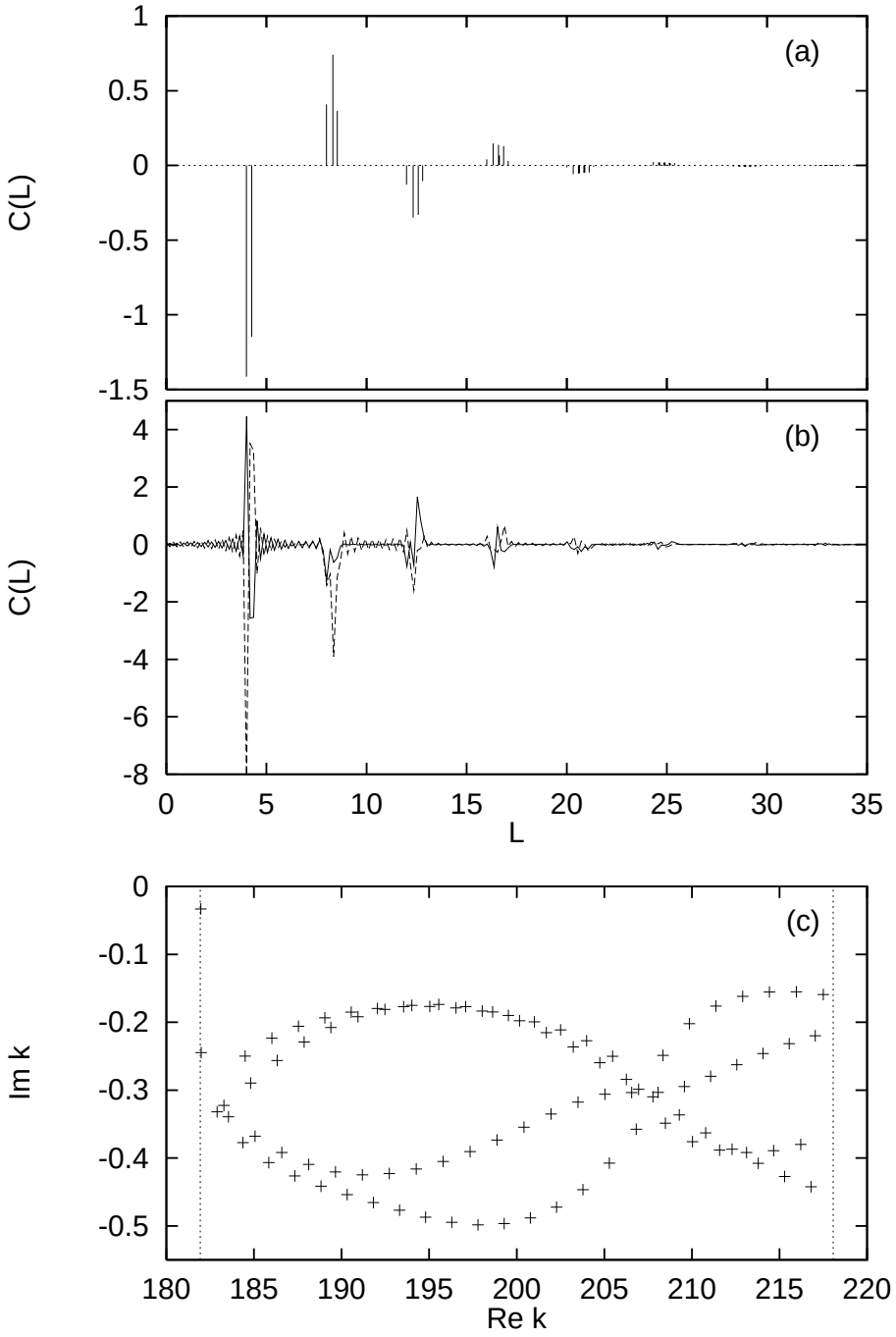

FIG. 1. (a) Periodic orbit recurrence signal for the three-disk scattering system with $R = 1$, $d = 6$ without filtering. The signal in the region $L \leq 35$ consists of 93 non-equidistant periodic orbit contributions (including multiple repetitions). (b) Same as (a) filtered with frequency window $w \in [182, 218]$. The band-limited signal consists of 201 equidistant data points with $\Delta L = 0.175$. The solid and dashed lines are the real and imaginary part of $C(L)$, respectively. (c) Semiclassical resonances obtained by harmonic inversion of the band-limited signal $C(L)$ in (b). The dotted lines mark the borders of the frequency window.

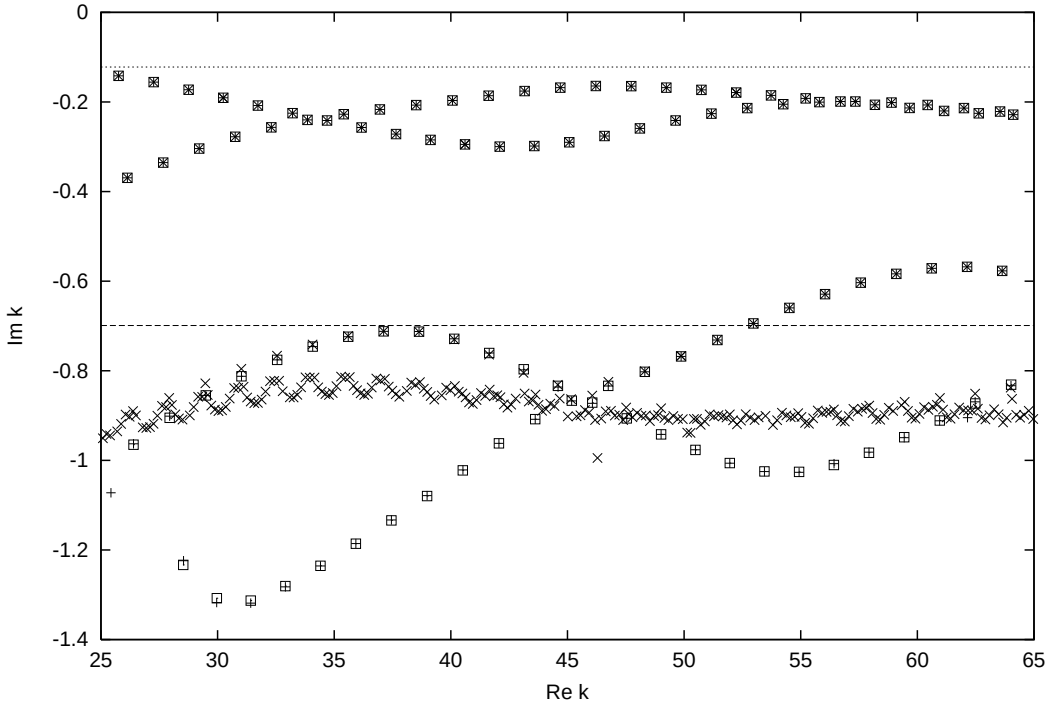

FIG. 2. Semiclassical resonances (A_1 subspace) for the three-disk scattering system with $R = 1$, $d = 6$. Squares: Harmonic inversion of the semiclassical recurrence signal; Plus symbols: Padé approximant to the periodic orbit sum; Crosses: Cycle expansion of the Gutzwiller-Voros zeta function [30]. The dotted and dashed lines mark the borderline for absolute convergence of Gutzwiller's trace formula (Im $k = -0.121\,557$) and the Gutzwiller-Voros zeta function (Im $k = -0.699\,110$), respectively. The Padé approximant and harmonic inversion results are found to converge deeper in the complex plane than do the Gutzwiller-Voros zeta function results.

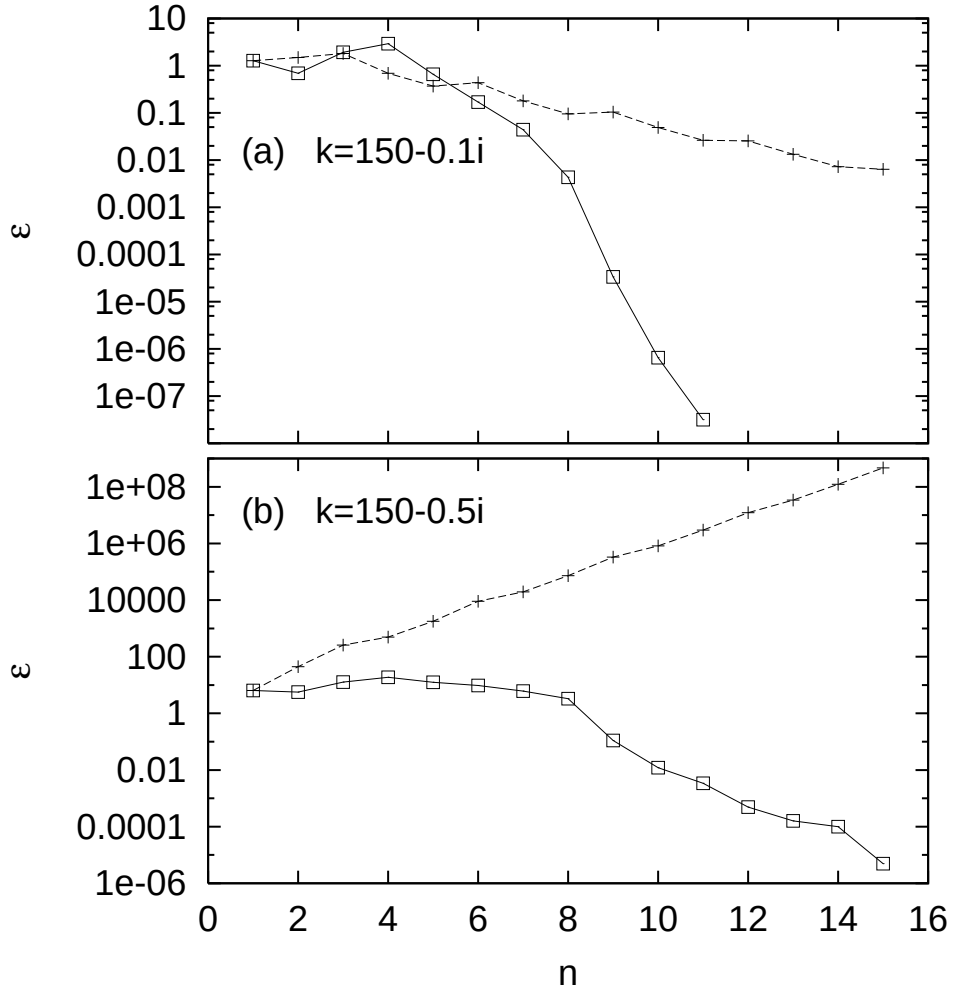

FIG. 3. Convergence vs. exponential divergence of the partial periodic orbit sums for the three-disk scattering system with $R = 1$, $d = 6$ as functions of the order n at (a) complex wave number $k = 150 - 0.1\mathrm{i}$ and (b) $k = 150 - 0.5\mathrm{i}$. Dashed lines and plus symbols: Error values $\varepsilon = |A_n - A_{n-1}|$ for the sequence A_n without Padé approximation. Solid lines and squares: Error values $\varepsilon = |A_n^{\mathrm{PA}} - A_{n-1}^{\mathrm{PA}}|$ for the Padé approximant to the periodic orbit sums.

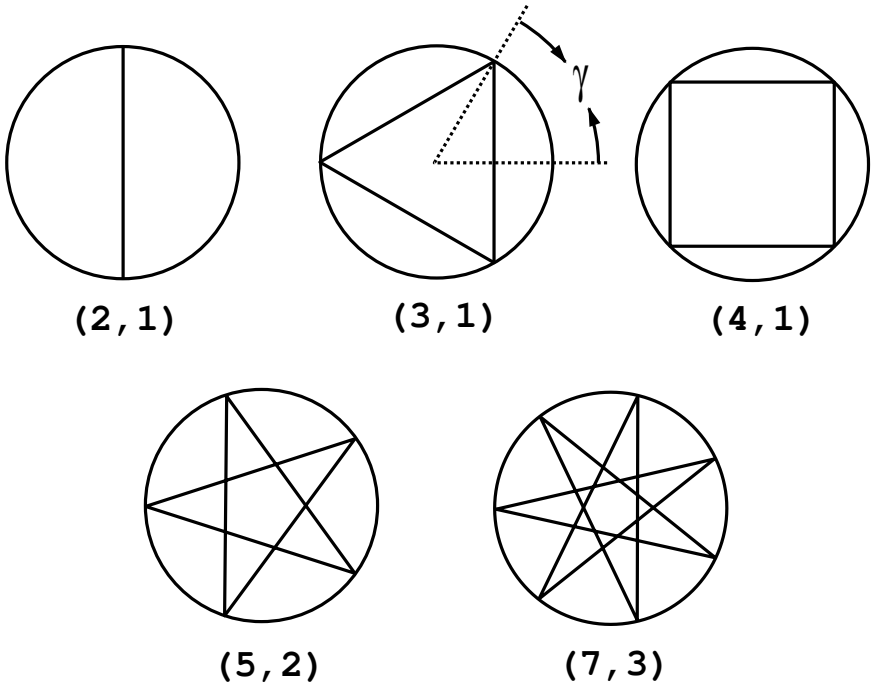

FIG. 4. Some examples of periodic orbits of the circle billiard. The orbits are labeled by the numbers (m_r, m_φ) which correspond to the number of sides of the polygons and the number of turns around the center. The angle γ is given by $\gamma = \pi m_\varphi / m_r$.

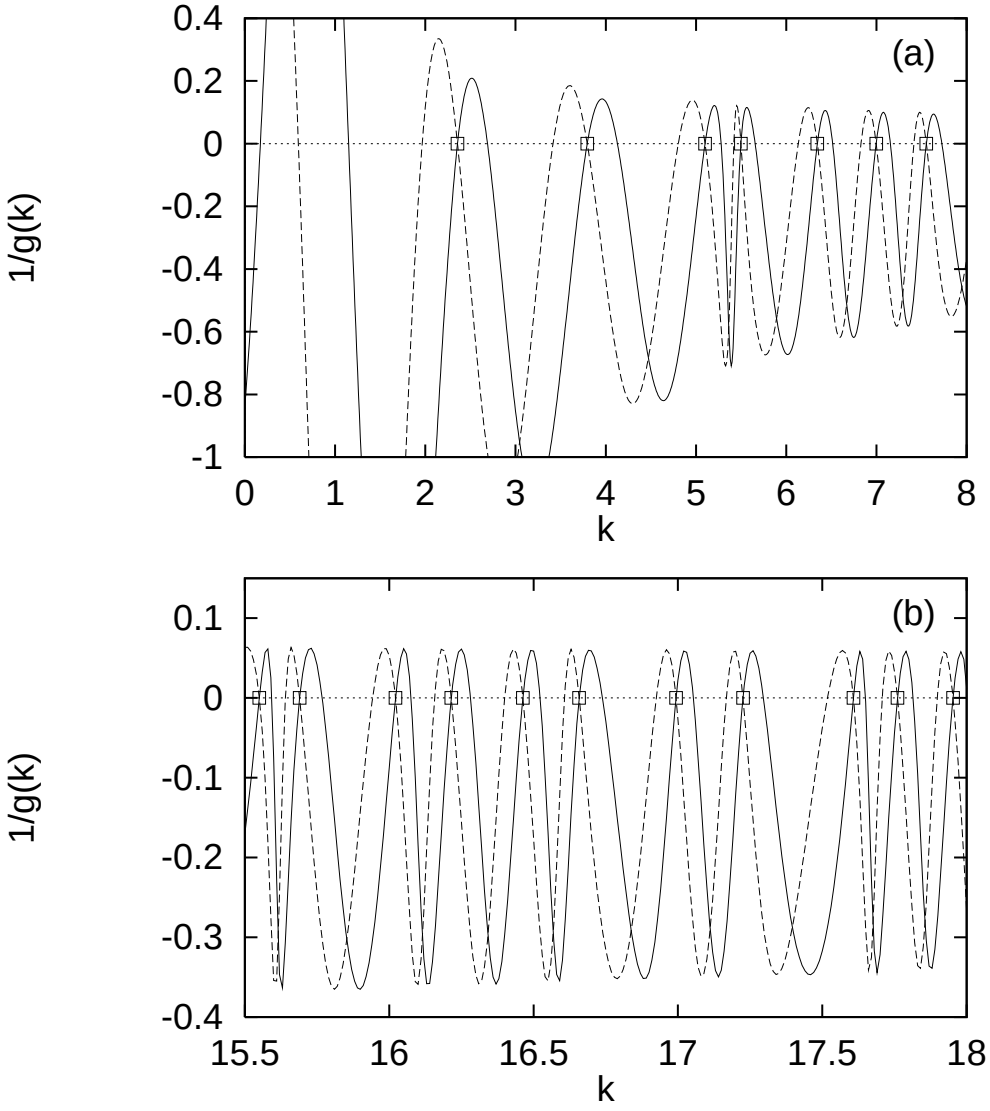

FIG. 5. Real part (solid line) and imaginary part (dashed line) of the function $1/g(k)$ for the circle billiard with radius $R = 1$ obtained by Padé approximant to the periodic orbit sum. The zeros agree perfectly with the exact positions of the semiclassical eigenvalues (from Eq. 36) marked by the squares.